

Journal of Applied and Natural Science

17(2), 720 - 731 (2025)

ISSN: 0974-9411 (Print), 2231-5209 (Online)

journals.ansfoundation.org

Research Article

Organic waste valorisation into biochar for the adsorptive removal of Malachite Green dye from its aqueous solution

Lata Verma

Department of Environmental Science, Babasaheb Bhimrao Ambedkar University, Lucknow- 226025 (Uttar Pradesh), India

Sarabjot Singh

School of Business, Faculty of Management, Shri Mata Vaishno Devi University,

Katra- 182320 (Jammu & Kashmir), India

Atin Kumar Pathak*

School of Energy Management, Shri Mata Vaishno Devi University,

Katra- 182320 (Jammu & Kashmir), India

Ashish Kumar

School of Energy Management, Shri Mata Vaishno Devi University,

Katra- 182320 (Jammu & Kashmir), India

Divya Singh Jamwal^{*}

School of Business, Faculty of Management, Shri Mata Vaishno Devi University,

Katra- 182320 (Jammu & Kashmir), India

Vinayak Vandan Pathak

Department of Sciences, Manav Rachna university, Faridabad (Haryana), India

*Corresponding author. E-mail: divyasinghjamwal@gmail.com

Article Info

https://doi.org/10.31018/ jans.v17i2.6236

Received: October 01, 2024 Revised: May 21, 2025 Accepted: May 28, 2025

How to Cite

Verma, L. et al. (2025). Organic waste valorisation into biochar for the adsorptive removal of Malachite Green dye from its aqueous solution. Journal of Applied and Natural Science, 17(2), 720 - 731. https://doi.org/10.31018/jans.v17i2.6236

Abstract

This study illustrated the biochar utilization as an adsorbent to remove the Malachite Green (MG) dye which is known to cause toxic and hazardous effects. The present research aimed to determine how well biochar adsorbs malachite green dye and comprehend the fundamental principles driving adsorption. The iron-impregnated biochar was synthesized using waste biomass of Teak (*Tectona speciose*), which is a timber tree, by pyrolysis process at 500 °C. The synthesized biochar was used to remove MG dye from a synthetically prepared MG solution to evaluate its adsorption efficiency. The bioadsorbent was characterized using Particle Size Analysis (PSA), Fourier Transform Infrared Spectroscopy (FTIR), Scanning Electron Microscopy (SEM), point of zero charges (pH_{ZPC}), Energy Dispersive X-ray (EDX). A batch adsorption experiment for the MG adsorption onto the MB-t surface was also conducted and it was found that the adsorption rate of MG was highly affected by the dose of biochar, temperature, working solution pH, time of contact and primary dye concentration. Isotherm study showed that the Temkin was the best-fit isotherm model to the adsorption process and the Q_{max} value was discovered to be 73.539 mg/g. Pseudo-second-order kinetics was best suited to the process of adsorption, indicating that the chemisorption was the rate-limiting factor. In contrast, the adsorption process was exothermic, which was determined through a thermodynamic study. The effective removal (89.05 %) of MG dye onto biochar (synthesized from Teak biomass the first time applied for dye removal) within 1 hr proved the bioadsorbent as a promising material for treating contaminated water.

Keywords: Adsorption, Biochar, Dye removal, Malachite green (MG)

INTRODUCTION

The production of synthetic dyes exceeds 2×10^5 metric tonnes annually due to the exponential growth in the use of several dye variations for a wide range of applications (Kumar *et al.*, 2021; Jabar *et al.*, 2023). Mala-

chite green (MG) is a synthetic organic substance based on triphenylmethane with stable chemical characteristics. It is a water-soluble and cationic dye that is used in several sectors like the textile industry's paper printing and dyeing operations (Islam *et al.*, 2023). However, MG and its metabolites, leucomalachite

green are extremely genotoxic and carcinogenic, and they can seriously harm humans, particularly the reproductive and immunological systems (Sinha et al., 2021; Wang et al., 2022). Meanwhile, it also negatively impacts important elements of soil ecosystems, which will majorly affect the soil and harm the ecosystem sooner or later. Several states have banned the use and dumping of of MG in marine ecosystems (Asif et al., 2024). In the mid-1990s, when MS was ultimately determined as hazardous and to be banned in seafood (Häder et al., 2020), their removal/ adsorption became more necessary.

Many physical processes have been developed to eliminate MG, including adsorption, filtration, nanofiltration, flocculation, ion exchange, and various other biological and chemical treatment techniques. Recently, the adsorption technique has been employed to use carbonbased nanomaterials to remove many hazardous environmental substances (Shukla et al., 2020; Asif et al., 2024). Researchers prefer adsorption because it is inexpensive. Adsorption has become a viable technique because it is simple to use, economical, and more effective at eliminating contaminants from water (Ajmal et al., 2020; Tony, 2022). Adsorbents are made from a variety of raw materials, including agricultural residues such as rice stalks, corn cobs, wheat stalks, rice husks. etc., plant residues and other organic wastes were used to remove several inorganic and organic impurities from water(Kumar and Ghosh, 2021).

Biochar is the carbon-rich material removed from the biomass and often pyrolyzed in an anaerobic environment (Verma and Singh, 2019). Due to its properties, such as large specific surface area, hydrophobic surface, porosity, and exceptional thermal stability, biochar has been investigated for decontaminating dyecontaining wastewater. It is a porous, carbon-enriched, and inexpensive substance produced through the thermal breakdown of organic biomass in an oxygen-limited environment (Akpasi et al., 2022). However, the magnetic biochar produced by pyrolyzing biomass and ferrates exhibits promising candidates for adsorption. A unique technique for modifying the surface characteristics of biochar and enhancing its sorption capacity is surface modification. Numerous investigations have demonstrated biochar's extraordinarily high pollutant removal capability enhanced by metal infusion, including Cu, Mn, Fe, Si, Ti, and Mg. Since Fe is a abundant natural resource and non-toxic to the environment, it is a desirable modifier to improve the properties of biochar (Premarathna et al., 2019; Qui et al., 2022; Asif et al., 2024). The aim of the present study was to investigate the efficiency of the magnetic biochar for the removal of malachite green dye from synthetically prepared dye solution in different conditions like concentration of dye, temperature influence, pH of the solution and amount of biochar used to remove MG-dye.

MATERIALS AND METHODS

Reagents and solution

Malachite Green ($C_{23}H_{25}CIN_2$; molecular wt.; 364.91 g/mol) was purchased from Thermo Fisher Scientific India Pvt. Ltd. and its stock solution was prepared in distilled water and further diluted to prepare a working solution as per the required concentration. 0.1 M Sodium hydroxide (NaOH) and Nitric acid (HNO₃) solutions were used to regulate the solution's pH. The standard and working solutions were stored in a dark place at ambient atmospheric temperature, i.e., 25 °C, Ferric chloride that was used for the iron-impregnated biochar was also brought from ThermoFisher Scientific (TFS), India Pvt. Ltd. The biomass waste for biochar synthesis was collected from the University campus.

Process of biochar synthesis and activation

The teak plant's organic waste was obtained from Babasaheb Bhimrao Ambedkar (BBA) University Lucknow, India. Subsequently, the collected wastes were washed at least three times with deionized water after being initially cleaned with tap water to remove any impurities that might have been there on the surface. After being cut into small pieces, the waste biomass was dried in a hot air oven at 105 °C for 24 hours to remove moisture. The dry waste biomass was then ground to obtain fibres of the same equal size. The resulting powdered biomass was then sieved with 250 µm mesh. After sieving the waste, biomass powder was used to produce biochar with magnetic properties. The process described by Sahu et al. (2022) was used to synthesise the biochar with magnetic properties after some modifications.

The FeCl₃ solution was prepared by adding 15 g of FeCl₃ to 150 mL of double distilled water and mixing 30 g of waste biomass powder into the FeCl₃ solution. This mixture was stirred with a magnetic stirrer for 60 minutes and kept in a hot air oven at 105 °C for 4 hours. After that, the mixture was filtered with a vacuum pump to remove excess FeCl₃ solution. Subsequently, this processed waste biomass material was pyrolyzed at 500 °C in a muffle furnace for 2 h. Before using teak magnetic biochar (MB-t) as a bio adsorbent to eliminate MG from the synthesized dye solution, it was washed again with double distilled water, then dried and ground homogenized and stored in a dry place.

Biochar characterization

The shape, size and structure of synthesized biochar were estimated using SEM (scanning electron microscope), and the elemental content of the biochar was characterized by using EDX (JOEL, JSM-6490 LV, Japan). Functional groups on MB-t were analysed using FTIR before and after adsorption of MG dye. The size

of the biochar particles was determined using Zeta Nanosizer (Nano ZS-90). The pH_{ZPC} was determined to evaluate the surface charge contained by the biochar. A pH meter was used to measure the pH of the solutions (Water analyser, *371*, Systronic).

Batch adsorption experiment

The batch adsorption study was carried out under variable conditions: Dose of bioadsorbent, primary concentration of the solution, pH of the solution, temperature and contact time of the adsorbent with the adsorbate. To determine the amount of MB-t, we added six different amounts, i.e., 0.1, 0.25, 0.5, 1.0, 1.25 and 1.5 g/L in a 20 mg/L of MG dye solution separately into Erlenmeyer flask of 250 mL capacity Erlenmeyer flask. The maximum adsorption of MG was achieved with a dose of 0.5 g/L, which was used for the rest of the MG sorption experiments. The concentration study involves different initial concentrations of the solution and in this study, 5, 10, 15, 20, 25, 30 and 35 mg/L were taken and for the temperature study, the different temperatures at which the experiment was conducted were 25 °C - 45 °C. The effect of pH (3-10 pH) and contact time (5-180 min) was also studied . The pH of the dye solution was maintained with HNO3 and NaOH solution at a concentration of 0.1 M and the pH of the dye solution was measured using a pH metre (Water Analyzer, 372 of Systronic, India Ltd.). The experiment was carried out with duplicate sets of samples to analyse the residual concentration of MG after adsorption. The residual concentration of MG after adsorption was determined at 620 nm using a wavelength UV-Vis spectrophotometer (117, Systronic India Ltd.). The equations for the percentage of removal and the adsorption capacity of the adsorbent were calculated by using the following equation:

Adsorption % =
$$\left(\frac{C_0 - C_t}{C_0}\right) \times 100$$
 Eq. 1

$$q_e \left(\frac{mg}{g}\right) = \frac{C_0 - C_e}{m} v$$
 Eq. 2

Here, C_t and C_0 are final dye concentration and initial MG concentration, correspondingly. The MB-t adsorbent capacity and final concentration of adsorbate were implied by qe and Ce. Volume of adsorbate was symbolised by v (litres) and mass of the MB-t was implied by m (g/L).

RESULTS AND DISCUSSION

Biochar characterization

Scanning Electron Microscope (SEM) and Energy Dispersive X-ray (EDX)

When the surface morphology structure was assessed using SEM, the result showed that the MB-t has an

asymmetrical shape and rough surface, as represented in Fig. 1a. Elemental composition of MB-t was analysed using EDX and the result showed that the carbon content was 42.8 % and 9.2 % of iron (Fig. 1b). This suggests that a significant amount of iron accumulates on the surface of the biosorbent, making magnetic biochar more efficient in removing malachite green dye from aqueous solutions with known dye concentrations. Similar results were reported in a study by Ibrahim *et al.* (2019), which found that biochar prepared at a higher temperature (500°C) had a higher iron content and a similar morphology.

pH at point zero charge (pH_{ZPC})

 pH_{ZPC} helps to define the net surface charge of the prepared biochar. The pH_{ZPC} of MB-t was discovered to be 2.8 (Fig.1c). The pH_{ZPC} represents the value at which the bioadsorbent exhibits zero surface charge, below which the bioadsorbent had positive surface charge and above that point, the bioadsorbent had a negative surface charge on it.

Particle size analysis (PSA)

The particle size of MB-t was examined by dispersing MB-t particles in a dispersing medium with pH 7. The result indicates that the size of MB-t was found to be between 140-190 nm and comes in the Micrometre category (Fig. 1d). Zhang *et al.* (2020) also reported the biochar particles were found in the range of 100 nm to 200 nm, which fall into the category of micrometer scale.

Fourier Transform Infra-red spectroscopy (FTIR)

Surface functional groups of MB-t were evaluated using FTIR from wavenumber 4000 to 400 cm⁻¹. Before adsorption of MG dye, numerous peaks were obtained at wavenumber 3600.4, 3390.2 and 3106.7 cm⁻¹ that, denoting the occurrence of hydroxyl group (-OH), the peak at 2913.9 cm⁻¹ and 2329.3 cm⁻¹ implies to CH₃ in aliphatic compound (Eltaweil et al., 2020). The peaks found at wavenumber 1498.4 cm⁻¹ were assigned to the carboxyl group (-COOH), although the peak found at 1135.8 cm-1 wavenumber resembles the O=C-O group. Aromatic hydrogen (C-H) groups were also present, which was confirmed by the peaks at wavenumbers 968.0 and 879 cm⁻¹ (Muinde et al., 2020). The peak at wavenumber 570.8 cm⁻¹ was due to the presence of a band of carboxylic group or Fe-O, whereas the C-N-C peak existed at wavenumber 474.4 cm⁻¹ that confirms the impregnation of iron into biochar (Verma et al., 2019).

After loading MG dye on MB-t biochar, the FTIR spectrum shows new peaks and the shifting of peaks. The FTIR data shows the occurrence of -OH bond at 3469.3 cm⁻¹ wavenumber, CH₃ in the aliphatic compound was found at the peak 2913.9 and 2329.3 cm⁻¹.

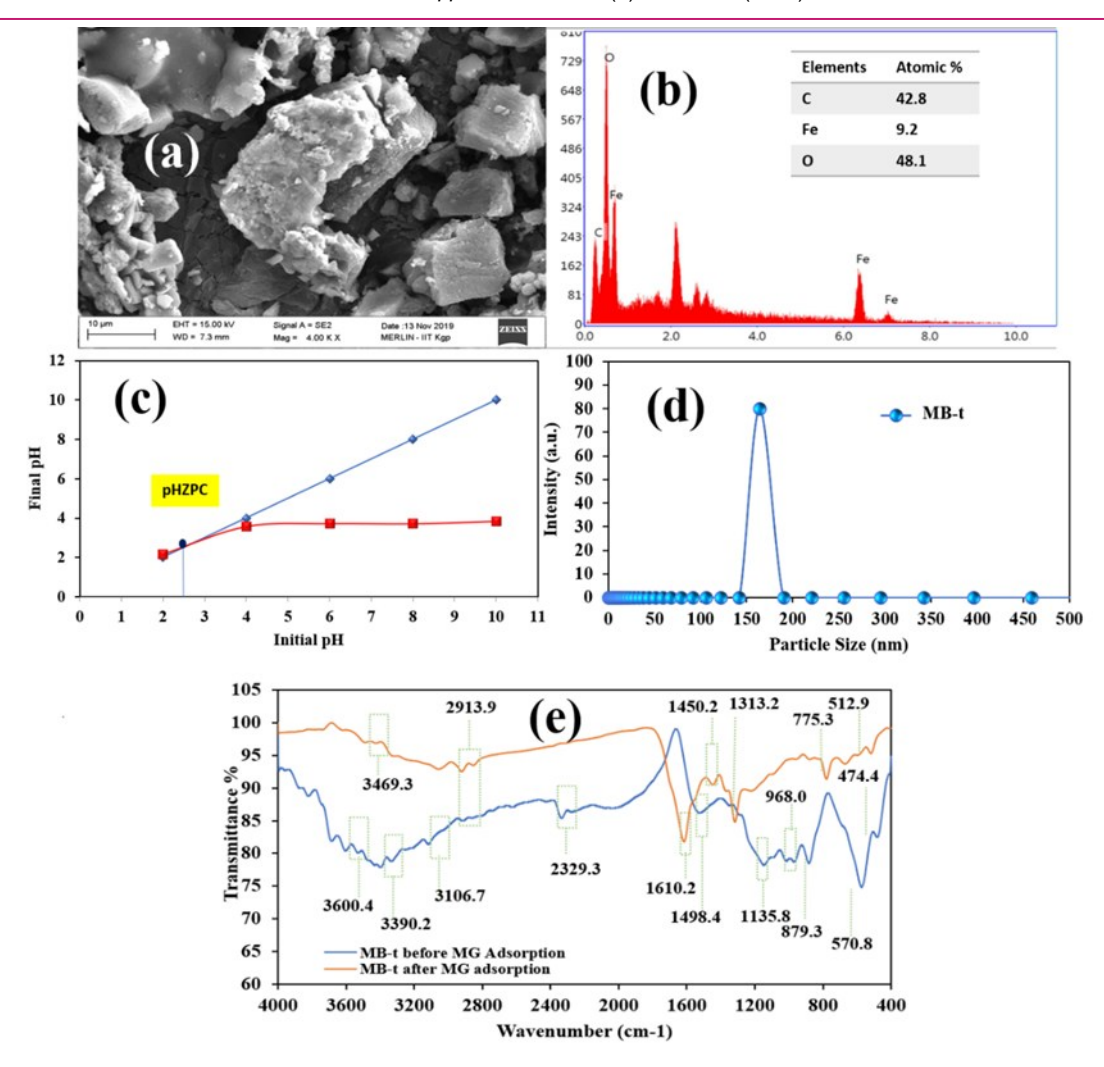


Fig. 1. a) SEM showing morphological structure of t-MB, b) EDX represents the elemental composition of t-MB, c) pH_{ZPC} of t-MB, d) PSA (particle size of MB-t) and e) FTIR showing surface functional groups of t-MB before and after adsorption of MG dye

The peak at 1610.2 and 1450.2 correspond to the C=C and carboxyl groups, respectively (Chen *et al.*, 2023). The peak at 1313.2 cm⁻¹ is assigned for N=N-O in azoxy compound. The peaks 775.3 and 512.9 cm-1 are attributed to the bending vibration of C-O bond and Fe-O group.

The peaks represent OH disappearing, or a decrease in intensity was observed after the adsorption of dye. The peak at 2329.3 cm⁻¹ also disappeared, and new peaks were found at wave numbers 1610.2 (C=C), 1313.2 (N=N-O), and 775.3 cm⁻¹ (C-O). The adsorption of MG on MB-t was confirmed by the appearance of new peaks, change in peak intensities, and shifting of peaks (1498.4 shifted to 1450.2) (Fig.1e). This could be because these functional groups are involved in the adsorption process. This behaviour of adsorption is similar with the results from other dye adsorption. In a study, activated biochar was used to remove MG dye, Wang *et al.* (2021) found comparable shifts in peaks, indicating the participation of functional groups on biochar surface, including hydroxyl, aromatic groups and

carboxyl groups in the adsorption process. These spectral alterations correspond to the claim that functional groups aid in binding the dye molecules and confirm the successful MG dye adsorption via biochar.

Batch adsorption Influence of biadsorbent dose

To determine the impact of the dose of bioadsorbent on MG dye sorption was done at 7 pH, 20 mg/L of initial dye concentration, the temperature was 25 □ with different bioadsorbent doses in the range of 0.1 to 1.5 g/L. Fig. 2a represents that the maximum adsorption of MG was 89.73 % achieved at 0.5 g/L of dose and the MB-t adsorption capacity was 4.10 mg/g at 0.5 g/L of dose. On further increasing the dose of MB-t a very small or nonexistence enhancement in the reduction of MG happened. The maximum adsorption capacity of MB-t for removal of MG was 36.12 mg/g and was decreased (1.88 mg/g) with increasing the concentration of dose (Fig. 2a). The removal percentage of dye was decreased with increased concentration of MB-t but be-

yond a certain point, adding more amount of biochar did not result in removing a greater amount of adsorbate. This was due to the agglomeration of MB-t particles into clusters, which reduces the surface area and active site for MG adsorption (Vigneshwaran *et al.*, 2021). Furthermore, Aziz *et al.* (2023) showed that the removal capacity decreased as the biochar concentration increased. The overlapping of adsorption sites explained this because of the agglomeration of the biochar, which results in reduced adsorption of dye molecules through biochar.

Influence of pH

Ionization of MG, surface charge on biochar and rate of adsorption all are greatly affected by the pH of the dye solution. As MG's stability changes with pH, it's pka (6.9) also affects how it behaves in the environment. As a result, the adsorption tests in the present study were conducted in the range pH 4 and 10 with the interval of 1. To study the influence of pH the experiment was performed with 0.5 g/L dose, baseline MG dye concentration was 20 mg/L while the temperature was 25 °C. This observation was made at pH 7 at which the maximum percentage absorption rate of 86.92 % was recorded for the dye as shown in Fig 2b. Alike result was also reported in research done by Amiri-Hosseini and Hashempour (2021); Eltaweil et a. (2020) in which maximum adsorption was obtained at pH and the minimum removal was found at lower pH or in an acidic medium.

It was observed that a change in the solution's pH resulted in various sorts of ions. The adsorbents' and the MG molecules' negatively charged surfaces grew as the pH level rose. Hence, a low value of elimination efficiency resulted from increased repulsive electrostatic interactions between the MB-t surface and MG dye, which was negatively charged. The maximum adsorption was achieved at pH 6 and the explanation for this trend, the higher H⁺ concentration at acidic (lower) pH enhanced the positive charge on MB-t surface, which instigates the repulsion among the positively charged biochar and MG dye (Chen et al., 2023). Inversely, as the pH of the solution rose to 6, the OH- groups or negative charge increased significantly on the MB-t surface; thus, the electrostatic attraction was increased amongst the positively charged MG and negatively charged biochar and the adsorption became favourable. pH_{ZPC} of the biochar was 2.3, indicating that the bioadsorbent had a negative surface charge beyond this point.

Influence of temperature on adsorption of MG

Temperature is an important factor that may greatly impact the adsorption process response rate. Every reaction condition, including net concentration, pH, and removal ability, was somewhat correlated with the sev-

eral temperatures. The temperature investigation was conducted at several temperatures, including 25, 35, 45, and 55 °C, while maintaining constant parameters (dose of 0.5 g/L, initial MG dye concentration of 20mg/L, and pH of 7). As demonstrated in Fig. 2c, it was discovered that the adsorption capacity reduced with increased temperatures and the percent removal of dye was also decreased on increased temperature from 25-55°C. The maximum adsorption of 86.92% at 25 °C was recorded when MB-t was utilized for the MG removal (Fig. 2c), and then the removal percentage decreased with increasing temperature to 82.88 % at 55 °C. This represents that MG removal from the aqueous solution by biosorbent is an exothermic process.

The active binding sites present on MB-t might not require very high temperatures, which improves the removal of MG dye at lower temperatures, whereas the breakdown of the active binding site on the MB-t surface or the desorption of MG molecules as an outcome of excessive heat availability may be the cause of the loss in adsorption capacity at higher temperatures (over 55 °C for MG adsorption, respectively) .As per Vergis et al. (2019), biochar materials are more efficient in removing MG-dye at lower or ambient temperatures, and their adsorption capacity declines with increased temperature. This was because higher temperatures restrict the adsorption efficiency by lowering the number of active sites on biochar surface.

Influence of initial dye concentration and time of contact

The influence of primary concentration on the removal of MG through MB-t was done at neutral pH, 0.5 g/L of dose, 25 °C temperature and different initial concentration of adsorbate i.e., in the range of 5 mg/L to 30 mg/L. Fig. 2d shows that MG adsorption was decreased with enhanced primary MG dye concentration. The maximum removal was 88.68 %, achieved at lower initial MG concentration, i.e., 5 mg/L. The adsorption was reduced from 88.68 % to 78.11 % on increasing primary dye concentration from 5mg/L to 30 mg/L. The value of adsorption capacity was increased with increasing concentration from 8.87 mg/g to 46.87 mg/g at 5 mg/L to 30 mg/L, correspondingly (Fig. 2e). The equilibrium was achieved in 60 min of contact time. As the primary MG dye concentration increased, the adsorption was reduced because the vacant active sites were saturated. This trend of adsorption was obtained may be due to the complete overload of MB-t active binding sites. The Fig. 2d also shows that, up to 60 minutes, the adsorption increases with time; however, no more increase in adsorption was observed after that. Initially, the number of molecules of MG dye was very low in the available active vacant sites of the adsorbent, so the adsorption was higher and was accessible for more adsorption of dye. The availability of vacant active

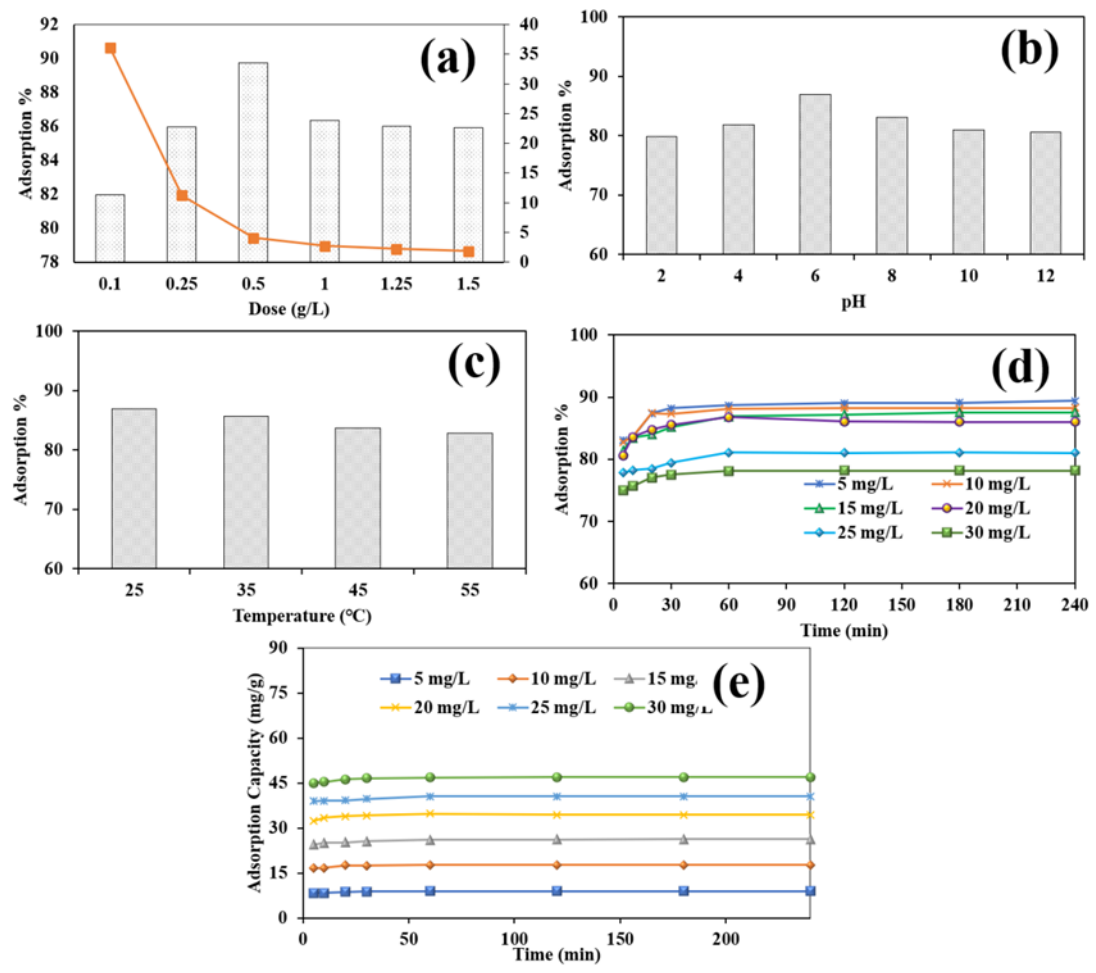


Fig. 2. Effect of a) Dose of MB-t along with adsorption capacity, b) pH of the solution, c) Temperature, d) Initial MG dye concentration and e) adsorption capacity of MB-t for MG adsorption

sites on biochar decreased with the increase in the initial concentration of dye. Similar results were also reported by Bensalah *et al.*(2020), Zubair *et al.*(2020), Khan *et al.* (2023).

Isotherm Study

An adsorption isotherm elaborates the adsorbents' equilibrium behaviour with their properties and pollutants removal from the aqueous medium. The isotherm models such as Freundlich, Temkin, and Langmuir were used to examine the best fit for the obtained equilibrium data.

Langmuir Isotherm

The effect of temperature experiments was conducted at four various temperatures from 25 to 55 °C , and with varying initial concentrations of MG between 5 to 40 mg/L. Every binding site of the MB-t has an equal affinity for the pollutant in a monolayer with homogeneous adsorption, as explained by the Langmuir adsorption model of isotherm (Hu *et al.*, 2023). Additionally, this model provides an equilibrium saturation point at which adsorption is terminated Eq. (3) provides the monolayer

adsorption model.

$$\frac{\textit{C}_e}{\textit{q}_e} = \frac{1}{\textit{qob}} + \frac{\textit{C}_e}{\textit{q}_0}$$
 Eq. 3

Where $C_{\rm e}$ and $q_{\rm e}$, are the final residual dye concentration after adsorption at the equilibrium point and adsorption capacity of MB-t at equilibrium point and the units are mg/L and mg/g units, separately. Q_0 (mg/g) and b (L/mg), are Langmuir's constants which highlighted the maximal adsorption capacity and rate of adsorption.

Meanwhile, plotting the plots between C_e/q_e versus C_e yields a $(1/Q_0)$ slope that resembled a straight line (Fig. 3a). For a Langmuir isotherm, the following equation represented the dimensionless separation factor:

$$RL = \frac{1}{1+bCo}$$
 Eq. 4

Here, b denotes the Langmuir adsorption equilibrium constant and the measuring unit is L/mg. C_0 (mg/L) is the solute's starting concentration, RL implied the dimensionless factor for Langmuir model. If the value of RL is greater than 1 the process is unfavourable, favourable if the value was greater than 0 and less than

1, linear when the value was equal to 1 and the adsorption process was irreversible if the value of RL was equal to 0. The graph of C_e/q_e against C_e 's slope and intercept was used to compute the b and Q_0 values. The linear graph confirmed the research's validity. MG is adsorbing favourably onto the MB-t based on the values of dimensionless constraint RL, which was found to be less than 1. Table 1 displays a plot of the calculated values of the Langmuir constant.

Freundlich isotherm

Adsorption that is both reversible and non-ideal is portrayed by the Freundlich model of adsorption isotherm (Musah *et al.*, 2022). This model was only applied for multilayer sorption (Heterogenous) with various binding energy spectra. The Freundlich isotherm equation is presented here in its linear format.

$$Log \ q_e = Log \ Kf + \frac{1}{n} Log \ C_e$$
 Eq. 5

Here, the adsorption capacity of MB-t is q_e (mg/g) at equilibrium, and the residual dye concentration is written as C_e (mg/L) at equilibrium. There are two constants for Freundlich isotherm: K_F and n. The process of sorption favouring or not favouring the Freundlich model of isotherm is shown by the value of n, while the ability of MB-t to adsorb MG on it is indicated by K_F (mg/g (L/mg)1/n). Plotting lnq_e versus lnC_e yields a value of 1/n (0 to 1), which represents the sorption amount and the heterogeneity of the MB-t surface (Fig. 3b). If ther value of 1/n is close to zero, the MB-t surface is considered more diverse or heterogenous. The obtained values of constant of Freundlich isotherm model is listed in Table 1.

Temkin isotherms

The impacts of MB-t and MG dye interactions during the process of adsorption were considered by the Temkin model of isotherm. The heat of adsorption of dye molecules in a layer reduces linearly with the coverage because of interaction of MB-t and MG dye molecules (Temkin & Pyzhev, 1940; Nandiyanto, 2020). This can be written as follows:

$$Qe = B \ln K_T + B \ln C_e$$
 Eq. 6

Here, the Temkin constant is presented by B, which is linked to the heat of sorption and maximal binding energy is attributed by K_T , which is Temkin binding constant. It is possible to determine the value of B and K_T from the graph obtained by q_e vs InC_e (Fig. 3c). All the values for Temkin constraints are tabulated in Table 1.

Adsorption isotherm study showed that R^2 value for Temkin isotherm is 0.985 and R^2 value for Langmuir isotherm was 0.758 with 73.54 mg/g Langmuir adsorption capacity. The correlation coefficient value for Freundlich model of isotherm is R^2 = 0.96. Results explained that Temkin isotherm was best fitted for the removal of MG by adsorbent (MB-t), which illustrates the heat of adsorption that decreased linearly with increasing coverage as per the electrostatic interaction between the adsorbate and adsorbent. Similar outcomes have also been reported by Ahmed *et al.*(2014) for the MG-dye through the process of adsorption.

According to the study's findings, the Temkin model more accurately depicted the actual adsorption process for MG dye on MB-t biochar than the Langmuir model, which suggested a finite number of adsorption sites. This is probably because of the surface heterogeneity of the biochar and the type of interactions that took place. On the other hand, the adsorption sites appear to be heterogeneous, having different affinities for the dye molecules, according to the Freundlich model, which has an R² value of 0.96.

Adsorption kinetics

The adsorption kinetics are crucial for the practical applicability of MB-t for MG dye removal. To assess the

Table 1. Isotherm parameters for Langmuir, Freundlich and Temkin models for MG dye removal with MB-t

Parameters	Value	
Q ₀ (mg/g)	73.539	,
B (L/mg)	0.274	
R_L	0.109	
R^2	0.9758	
K_F (mg/g(L/mg)1/n)	3.027	
1/n	1.497	
R^2	0.96	
В	15.634	
K _⊤ (L/mg)	2.964	
b_T (kJ/mol)	1.086	
R^2	0.985	
	$\begin{array}{c} Q_0 \ (mg/g) \\ B \ (L/mg) \\ R_L \\ R^2 \\ K_F \ (mg/g(L/mg)1/n) \\ 1/n \\ R^2 \\ B \\ K_T \ (L/mg) \\ b_T \ (kJ/mol) \end{array}$	$\begin{array}{cccccccccccccccccccccccccccccccccccc$

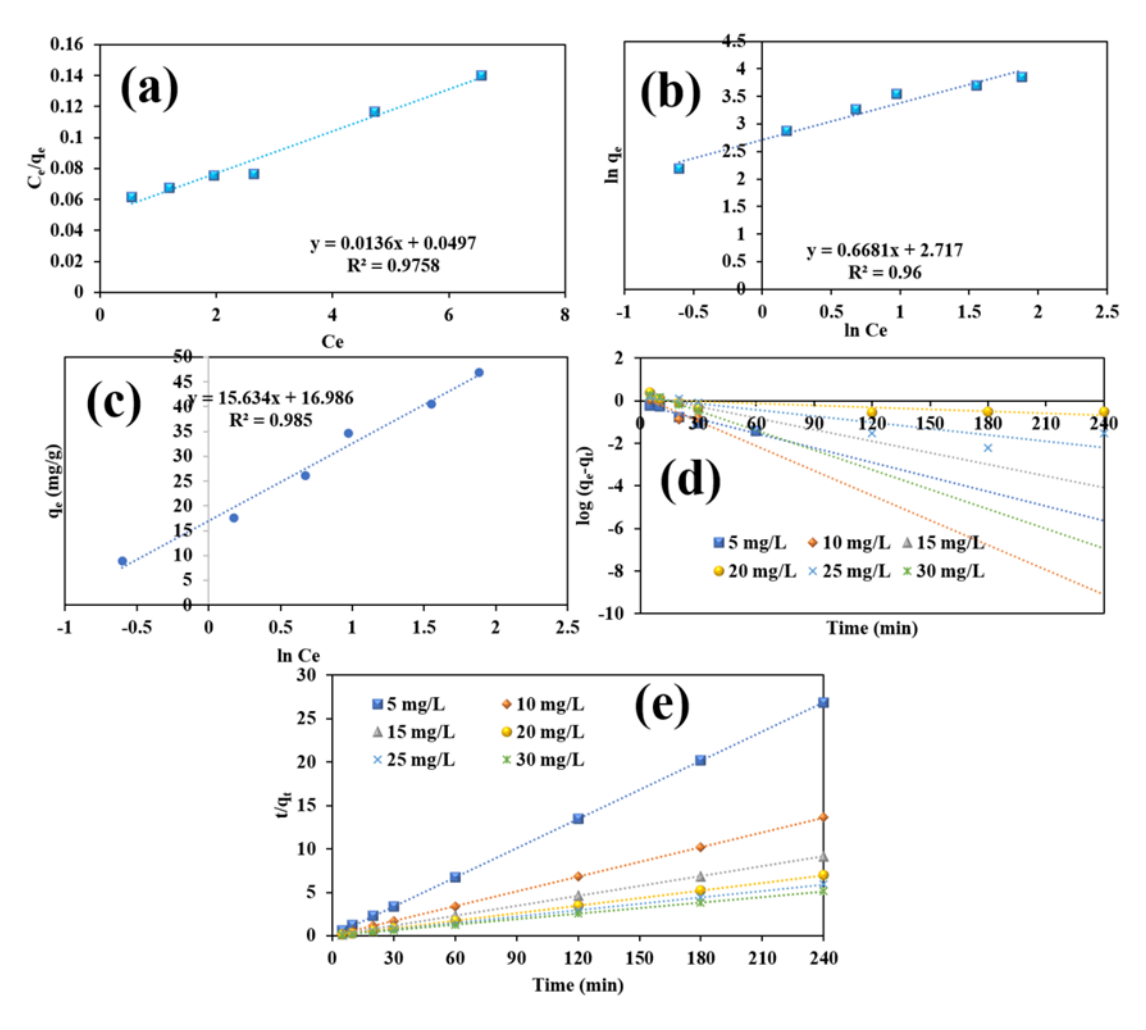


Fig. 3. a) Langmuir isotherm, b) Freundlich isotherm, c) Temkin isotherm model, d) Pseudo-first-order kinetics and e) Pseudo-second-order kinetics for MG removal

adsorption kinetics pseudo-first-order and pseudo-second-order kinetics models were used.

Equation 7 is used to calculate the values of pseudo-first-order kinetic (Verma et al., 2022).

$$log(q_e - q_t) = log q_e - \left(\frac{k_1}{2.303}\right)$$
 Eq. 7

Where q_e = adsorbed MG at equilibrium, q_t = adsorbed quantity of MG at time and K_1 is the rate constant. The K1, qe and qt values were calculated at every concentration as presented in Table 2. Meanwhile, the graph was plotted amongst the values of ln(qe-qt) and t to calculate the value of K_1 (Fig. 3d).

The pseudo-second-order (Goddeti et al., 2020) is explained below.

$$rac{t}{q_t} = rac{1}{(k_2q_e^2)} + \left(rac{1}{q_e}
ight) t$$
 Eq. 8

Here, the pseudo-second-order kinetic (K2) rate constant was estimated from the graph of t/q_t vs t (Fig. 3e) and their computed values are given in Table 2. The

experimental data was best fitted with the pseudo-second-

order kinetic model with correlation coefficient value (R²= 1) for MG adsorption using MB-t, indicating that the rate-limiting step is chemisorption. It was observed that the pseudo-first-order kinetics were not fitted to the experimental data of MG dye adsorption through MB-t biochar and all the calculated values for pseudo-first-order and pseudo-second-order are given in Table 2.

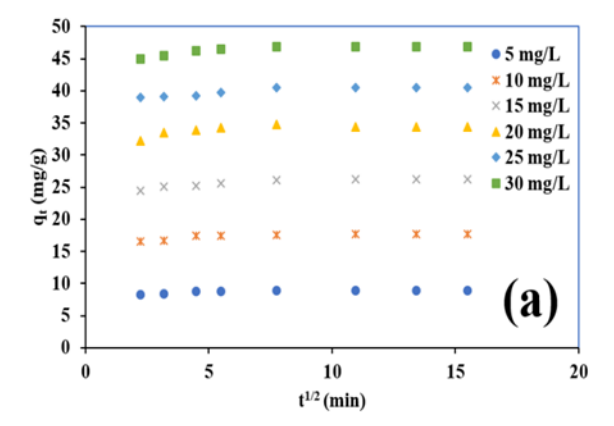
Wang et al. (2021) also reported a similar result in which they used agricultural waste for biochar synthesis for MG-dye removal and found that the adsorption process is controlled by chemical interactions between the adsorbent and adsorbate as the adsorption process best fitted to the pseudo-second-order. Overall, this study's excellent fit of the pseudo-second-order model was a clear sign that the MG dye molecules and the biochar surface formed a chemical interaction during adsorption.

Intra-particle diffusion model (IPDM)

The Intra-Particle Diffusion Model (IPDM) outlines the

Table 2. Value of kinetics parameter for MG removal using MB-t

C ₀ (mg/L)	Pseud-first-order kinetics			Pseudo-sec	Pseudo-second-order kinetics		
	q₀ (mg/g)	k₁ (min-1)	\mathbb{R}^2	q _e (mg/g)	k ₂ (g/(mg min))	R ²	
5	0.660	0.010	0.9061	8.953	0.209	1	
10	1.607	0.017	0.7909	17.668	0.168	1	
15	1.843	800.0	0.9344	26.316	0.056	1	
20	1.127	0.001	0.6377	34.483	0.172	1	
25	1.426	0.004	0.8195	40.650	0.061	1	
30	2.782	0.013	0.9955	46.948	0.086	1	



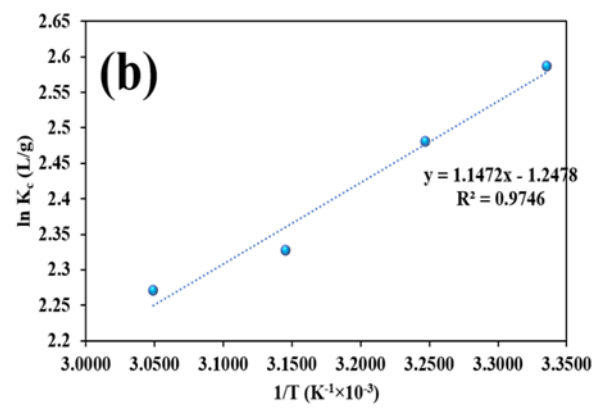


Fig. 4. Graph of a) Intraparticle diffusion model and b) Thermodynamics for the MG dye adsorption using MB-t.

three stages involved in the sorption of a contaminant onto the MB-t surface. Firstly, the adsorbate is adsorbed onto the MB-t surface through the external surface, or prompt adsorption process; secondly, there is steady adsorption, which illustrates controlled intraparticle diffusion; and thirdly, the adsorbate transfers from larger pore to micropores, resulting in a decrease in the adsorption rate and, ultimately, reaching the equilibrium step (Muinde et al., 2020). This process is represented by the IPDM, which was anticipated by Weber and Morris, (1963) via Eq. given below:

$$q_t = k_i t^{1/2} + C$$
 Eq. 9

Here, Ki= rate constant for the intraparticle diffusion (mg g⁻¹ min⁻¹)

C= boundary layer thickness (mg g⁻¹)

The values of C and K_i are computed from the values of slope and intercept of q_t vs. $t^{1/2}$ plots (Fig. 4a) respectively. Plotting q_t vs $t^{1/2}$ shows

that the origin is passed through if the solute's adsorption is regulated by the intra-particle diffusion mechanism, as per IPDM. Thus, it was determined that the MG dye adsorption onto MB-t is facilitated by intraparticle diffusion.

Thermodynamics

Thermodynamics study was performed to determine the temperature favourability on adsorption of MG dye.

Gibb's free energy (ΔG°), enthalpy (ΔH°) and entropy (ΔS°) are the three main components of thermodynamics. The computation of these constraints of thermodynamics was performed using following Eq:

$$K_C = \frac{q_e}{c_e}$$
 Eq. 10

$$lnK_C = \frac{\Delta S}{R} - \frac{\Delta H}{RT}$$
 Eq. 11

$$\Delta G^{\circ} = -RT \ lnK_c$$
 Eq. 12

Where, initial MG dye concentration (mg/L) and quantity of dye get adsorbed by the MB-t (mg/g) is denoted by C_e and q_e , correspondingly at equilibrium point. K_c stands for the thermodynamic constant, 8.314 J/mol K is the gas constant value and is denoted by R and T (K) stands for absolute temperature. The value of all three parameters of the thermodynamics were calculated by plotting the graph (Fig. 4b) between the values of InK_c and 1/T (Table 3).

The result of thermodynamics shows that the adsorption of MG dye was decreased with increasing temperature that depicts the adsorption is exothermic and the same was confirmed by the positive value of ΔG° , i.e., 3.08, 3.19, 3.29, 3.39 kJ for 25, 35, 45 and 55 \square , respectively, the positive value of Gibb's free energy shows the non-spontaneous process of adsorption for

Table 3. Parameters of thermodynamic study for MG adsorption using MB-t biochar

Tempera- ture (K)	Thermodynamics parameters					
	ΔG (kJ/mol)	ΔH (kJ/mol)	ΔS (J/mol K)			
298	3.082	-9.54	-10.37			
308	3.186					
318	3.289					
328	3.393					

MG removal using MB-t. The value of ΔH° (-9.54 J/mol K) and ΔS° (-10.37 J/mol K) are negative and that revealed the good affinity of MB-t for MG removal (Eltaweil *et al.*, 2020). These thermodynamic parameters provide more evidence that the adsorption of MG dye on MB-t biochar is an exothermic, nonspontaneous process that happens when the temperature drops and the dye molecules have a strong affinity for the biochar surface, as shown by the negative values of ΔH° and ΔS° .

These results are consistent with earlier research that used biochar to adsorb MG dye, namely Eltaweil *et al.* (2020), which obtained similar thermodynamic results. The exothermic character of the adsorption process was also demonstrated by the study's negative values of ΔH° and ΔS° , which showed that the system's randomness decreased as the dye was adsorbed. Furthermore, as is common for exothermic reactions, the positive values of ΔG° seen in both investigations verify that the adsorption process for MG elimination is not spontaneous and necessitates an external energy input.

Conclusion

The present study proved that MB-t had a greater efficacy in removing MG dye from an aqueous of its known concentration and can be utilised for the adsorption of MG from contaminated water in future industrial applications. EDX analysis revealed that the material is successfully infused with iron, making the adsorbent magnetic and easily recovers using a magnetic field. The biochar particle size was found in the 140-190 nm scale. The maximum adsorption was 89.73 % achieved with 0.5 g/L of dose. The highest MG sorption occurred at pH 6, and the equilibrium time for MG adsorption was achieved within 60 minutes of contact time. The adsorption percentage was 88.68 % at 5 mg/L dye concentration and reduced with increased (30 mg/L) primary concentration of dye. The q_{max} value was 73.539 mg/ g, which was obtained from Langmuir model of isotherm calculation. Pseudo-second-order kinetics shows the greatest fit for the adsorption data, which revealed that the process of adsorption is chemisorption, which was the rate-limiting factor. Intraparticle diffusion was

not the only controlling factor in the adsorption of MG dye from synthetically prepared dye solution as the trendlines did not pass the origin. Thermodynamic study shows the non-spontaneous process of Dye adsorption onto MB-t surface. FTIR results illustrated that various function groups of the surface of biochar were required to eliminate MG dye from synthetically prepared dye solution. The overall study concluded that this biochar can be the best alternative to the expensive adsorbents commercially available in the market for treating water contaminated with dye.

Conflict of interest

The authors declare that they have no conflict of interest.

REFERENCES

- Ajmal, Z., Muhmood, A., Dong, R., & Wu, S. (2020). Probing the efficiency of magnetically modified biomass-derived biochar for effective phosphate removal. *Journal of Environmental Management*, 253, 109730. https://doi.org/10.1016/j.jenvman.2019.109730
- Akpasi, S. O., Anekwe, I. M. S., Adedeji, J., & Kiambi, S. L. (2022). Biochar development as a catalyst and its application. In Biochar-Productive Technologies, Properties and Applications. *IntechOpen*. https://doi.org/10.5772/intechopen.105439
- Amiri-Hosseini, S., & Hashempour, Y. (2021). Photocatalytic removal of Malachite green dye from aqueous solutions by nano-composites containing titanium dioxide: A systematic review. *Environmental Health Engineering and Management Journal*, 8(4), 295-302. https://doi.org/10.34172/EHEM.2021.33
- Asif, H., Munir, R., Albasher, G., Sayed, M., Muneer, A., Mansha, A., & Noreen, S. (2024). Fabrication of green magnetized ferrite biochar nanocomposites from orange peels/MnFe2O4, peanut shells/CuFe2O4, tree twigs/Ni Fe2O4, and wood/CoFe2O4: characterization and application as adsorbents for adsorption/desorption/stability of basic Blue-XGRRL dye with possible mechanisms. AQ-UA—Water Infrastructure, Ecosystems and Society, 73(2), 217-238. https://doi.org/10.2166/aqua.2024.266
- Aziz, S., Uzair, B., Ali, M. I., Anbreen, S., Umber, F., Khalid, M., & Tambuwala, M. M. (2023). Synthesis and characterization of nanobiochar from rice husk biochar for the removal of safranin and malachite green from water. *Environmental Research*, 238, 116909. https://doi.org/10.1016/j.envres.2023.116909
- Bensalah, H., Younssi, S. A., Ouammou, M., Gurlo, A., & Bekheet, M. F. (2020). Azo dye adsorption on an industrial waste-transformed hydroxyapatite adsorbent: Kinetics, isotherms, mechanism and regeneration studies. *Journal* of *Environmental Chemical Engineering*, 8(3), 103807. https://doi.org/10.1016/j.jece.2020.103807
- Chen, L., Mi, B., He, J., Li, Y., Zhou, Z., & Wu, F. (2023). Functionalized biochars with highly-efficient malachite green adsorption property produced from banana peels via microwave-assisted pyrolysis. *Bioresource Technology*, 376, 128840. https://doi.org/10.1016/j.biortech.20 23.128840

- Eltaweil, A. S., Mohamed, H. A., Abd El-Monaem, E. M., & El-Subruiti, G. M. (2020). Mesoporous magnetic biochar composite for enhanced adsorption of malachite green dye: Characterization, adsorption kinetics, thermodynamics and isotherms. *Advanced Powder Technology*, 31(3), 1253-1263. https://doi.org/10.1016/ j.apt.2020.01.005
- Goddeti, S. M. R., Bhaumik, M., Maity, A., & Ray, S. S. (2020). Removal of Congo red from aqueous solution by adsorption using gum ghatti and acrylamide graft copolymer coated with zero valent iron. *International Journal of Biological Macromolecules*, 149, 21-30. https:// doi.org/10.1016/j.ijbiomac.2020.01.099
- Häder, D. P., Banaszak, A. T., Villafañe, V. E., Narvarte, M. A., González, R. A., & Helbling, E. W. (2020). Anthropogenic pollution of aquatic ecosystems: Emerging problems with global implications. Science of the Total Environment, 713, 136586. https://doi.org/10.1016/ j.scitotenv.2020.136586
- Hu, Q., Lan, R., He, L., Liu, H., & Pei, X. (2023). A critical review of adsorption isotherm models for aqueous contaminants: Curve characteristics, site energy distribution and common controversies. *Journal of Environmental Management*, 329, 117104. https://doi.org/10.1016/ j.jenvman.2022.117104
- Ibrahim M, Siddiqe A, Verma L, Singh J, Koduru JR (2019) Adsorp tive removal of fluoride from aqueous solution by biogenic iron permeated activated carbon derived from sweet lime waste. Acta Chim Slov 66:123–136
- Islam, T., Repon, M. R., Islam, T., Sarwar, Z., & Rahman, M. M. (2023). Impact of textile dyes on health and ecosystem: A review of structure, causes, and potential solutions. *Environmental Science and Pollution Research*, 30 (4), 9207-9242. https://doi.org/10.1007/s11356-022-24398-3
- 14. Jabar, J. M., Adebayo, M. A., Odusote, Y. A., Yılmaz, M., & Rangabhashiyam, S. (2023). Valorization of microwave -assisted H3PO4-activated plantain (Musa paradisiacal L) leaf biochar for malachite green sequestration: models and mechanism of adsorption. Results in Engineering, 18, 101129. https://doi.org/10.1016/j.rineng.2023.101129
- Khan, F. A., Dar, B. A., & Farooqui, M. (2023). Characterization and adsorption of malachite green dye from aqueous solution onto Salix alba L. (Willow tree) leaves powder and its respective biochar. *International Journal of Phytoremediation*, 25(5), 646-657. https://doi.org/10.1080/15226514.2022.2098909
- Kumar, A., & Ghosh, A. K. (2021). Assessment of arsenic contamination in groundwater and affected population of Bihar. Arsenic Toxicity: Challenges and Solutions, 165-191. https://doi.org/10.1007/978-981-33-6068-6_7
- Kumar, B., Agrawal, K., & Verma, P. (2021). Microbial electrochemical system: a sustainable approach for mitigation of toxic dyes and heavy metals from wastewater. *Journal of Hazardous, Toxic, and Radioactive Waste*, 25(2), 04020082. https://doi.org/10.1061/(ASCE)HZ.2153-5515.0000590
- Muinde, V. M., Onyari, J. M., Wamalwa, B., & Wabomba, J. N. (2020). Adsorption of malachite green dye from aqueous solutions using mesoporous chitosan–zinc oxide composite material. *Environmental Chemistry and Ecotoxicology*, 2, 115-125. https://doi.org/10.1016/

- j.enceco.2020.07.005
- Musah, M., Azeh, Y., Mathew, J. T., Umar, M. T., Abdulhamid, Z., & Muhammad, A. I. (2022). Adsorption kinetics and isotherm models: a review. *CaJoST*, 4(1), 20-26. https://doi.org/DOI:10.4314/cajost.v4i1.3
- Nandiyanto, A. B. D. (2020). Isotherm adsorption of carbon microparticles prepared from pumpkin (Cucurbita maxima) seeds using two-parameter monolayer adsorption models and equations. *Moroccan Journal of Chemistry*, 8(3), 745-761. https://doi.org/10.48317/IMIST.PRSM/morjchem-v8i3.21636
- Premarathna, K. S. D., Rajapaksha, A. U., Sarkar, B., Kwon, E. E., Bhatnagar, A., Ok, Y. S., & Vithanage, M. (2019). Biochar-based engineered composites for sorptive decontamination of water: A review. *Chemical Engineering Journal*, 372, 536-550. https://doi.org/10.1016/j.cej.2019.04.097
- Qiu, M., Liu, L., Ling, Q., Cai, Y., Yu, S., Wang, S., & Wang, X. (2022). Biochar for the removal of contaminants from soil and water: a review. *Biochar*, 4(1), 19. https://doi.org/10.1007/s42773-022-00146-1
- Sahu, N., Nayak, A. K., Verma, L., Bhan, C., Singh, J., Chaudhary, P., & Yadav, B. C. (2022). Adsorption of As (III) and As (V) from aqueous solution by magnetic biosorbents derived from chemical carbonization of pea peel waste biomass: Isotherm, kinetic, thermodynamic and breakthrough curve modeling studies. *Journal of Environmental Management*, 312, 114948. https://doi.org/10.1016/j.jenvman.2022.114948
- 24. Shukla, K., Verma, A., Verma, L., Rawat, S., & Singh, J. (2020). A novel approach to utilize used disposable paper cups for the development of adsorbent and its application for the malachite green and rhodamine-B dyes removal from aqueous solutions. *Nature Environment & Pollution Technology*, 9(1), 57-70.
- Sinha, R., Jindal, R., & Faggio, C. (2021). Protective effect of Emblica officinalis in Cyprinus carpio against hepatotoxicity induced by malachite green: ultrastructural and molecular analysis. *Applied sciences*, 11(8), 3507. https:// doi.org/10.3390/app11083507
- Temkin I., & Pyzhev V. (1940). Kinetics of ammonia synthesis on promoted iron catalysts. *Acta Physics Chimica*, 12, 327–356
- Tony, M. A. (2022). Low-cost adsorbents for environmental pollution control: a concise systematic review from the prospective of principles, mechanism and their applications. *Journal of Dispersion Science and Technology*, 43 (11), 1612-1633. https://doi.org/10.1080/019326 91.2021.1878037
- Vergis, B. R., Kottam, N., Krishna R. H., & B. M. Nagabhushana (2019). Removal of Evans Blue dye from aqueous solution using magnetic spinel ZnFe2O4 nanomaterial: adsorption isotherms and kinetics. *Nanostructures and Nano-objects*, 18, 100290. https://doi.org/10.1016/j.nanoso.2019.100290
- Verma, L., & Singh, J. (2019). Synthesis of novel biochar from waste plant litter biomass for the removal of Arsenic (III and V) from aqueous solution: A mechanism characterization, kinetics and thermodynamics. *Journal of Environmental Management*, 248, 109235. https://doi.org/10.1016/j.jenvman.2019.07.006
- 30. Verma, L., Siddique, M. A., Singh, J., & Bharagava, R. N.

- (2019). As (III) and As (V) removal by using iron impregnated biosorbents derived from waste biomass of Citrus limmeta (peel and pulp) from the aqueous solution and ground water. *Journal of environmental management*, 250, 109452. https://doi.org/10.1016/j.jenvman.2019.109452
- Verma, L., Sonkar, D., Bhan, C., Singh, J., Kumar, U., Yadav, B. C., & Nayak, A. (2022). Adsorptive performance of Tagetes flower waste-based adsorbent for crystal violet dye removal from an aqueous solution. *Environmental* Sustainability, 5(4), 493-506. https://doi.org/10.1007/ s42398-022-00250-9
- 32. Vigneshwaran, S., Sirajudheen, P., Karthikeyan, P., & Meenakshi, S. (2021). Fabrication of sulfur-doped biochar derived from tapioca peel waste with superior adsorption performance for the removal of Malachite green and Rhodamine B dyes. *Surfaces and Interfaces*, 23, 100920. https://doi.org/10.1016/j.surfin.2020.100920
- Wang, P., Chen, W., Zhang, R., & Xing, Y. (2022). Enhanced removal of malachite green using calcium-functionalized magnetic biochar. *International journal of environmental research and public health*, 19(6), 3247.

- https://doi.org/10.3390/ijerph19063247
- Wang, X., Zhang, Y., & Liu, X. (2021). Removal of malachite green dye from aqueous solutions using biocharbased adsorbents: A review. Journal of Environmental Management, 287, 112284. https://doi.org/10.1016/j.jenvman.2021.112284.
- Weber, W.J., & Morris, J.C. (1963). Kinetics of adsorption on carbon from solution. *Journal of the Sanitary Engineer*ing Division, American Society of Civil Engineers, 89, 31– 59. https://doi.org/10.1061/JSEDAI.0000430
- 36. Zubair, M., Mu'azu, N. D., Jarrah, N., Blaisi, N. I., Aziz, H. A., & A. Al-Harthi, M. (2020). Adsorption behavior and mechanism of methylene blue, crystal violet, eriochrome black T, and methyl orange dyes onto biochar-derived date palm fronds waste produced at different pyrolysis conditions. Water, Air, & Soil Pollution, 231, 1-19. https://doi.org/10.1007/s11270-020-04595-x
- Zhang, X., Zhang, P., Yuan, X., Li, Y., & Han, L. (2020). Effect of pyrolysis temperature and correlation analysis on the yield and physicochemical properties of crop residue biochar. *Bioresource technology*, 296, 122318. https:// doi.org/10.1016/j.biortech.2019.122318